

Original Research Article

Effects of Different Fluting Medium Geometries on Von-Mises Stress and Deformation in Single Fluted Board: A Three-Dimensional Finite Element Analysis

Mohd Salahuddin Mohd Basri^{1,2,3*}, Mohd Zuhair Mohd Nor^{1,2}, Rosnah Shamsudin^{1,2}, Intan Syafinaz Mohamed Amin Tawakkal^{1,2}, Nur Hamizah Abdul Ghani¹, Khairul Manami Kamarudin⁴, Anas Mohd Mustafah⁵

¹Department of Process and Food Engineering, Faculty of Engineering, Universiti Putra Malaysia, 43400 Serdang, Selangor, Malaysia.

²Laboratory of Halal Science Research, Halal Products Research Institute, Universiti Putra Malaysia, 43400 Serdang, Malaysia

³Laboratory of Biopolymer and Derivatives, Institute of Tropical Forestry and Forest Products (INTROP), Universiti Putra Malaysia, Serdang 43400, Selangor, Malaysia

⁴Department of Industrial Design, Faculty of Design and Architecture, Universiti Putra Malaysia, 43400 Serdang, Selangor, Malaysia.

⁵Department of Biological and Agricultural Engineering, Faculty of Engineering, Universiti Putra Malaysia, 43400 Serdang, Selangor, Malaysia.

*Corresponding author: Mohd Salahuddin Mohd Basri, Department of Process and Food Engineering, Faculty of Engineering, Universiti Putra Malaysia, 43400 Serdang, Selangor, Malaysia; salahuddin@upm.edu.my

Abstract: Paperboard box produced in large volume for packaging purpose either to pack light or heavy product. When a heavy product is packed, high strength and structural stability against compression and deformation of the paperboard box are demanded. This paper investigates the effects of different shape of fluting mediums on the von Mises stress and deformation using finite element analysis (FEA) tool. Solidworks and ANSYS software were used to design a 3-D model and perform static structural analysis, respectively. The result from the analysis and simulation revealed that common s-shape geometry experienced the lowest von Mises stress and deformation. Honeycomb geometry experienced the highest von Mises stress of 0.19576 MPa while triangle fluting medium recorded the highest deformation at $1.8695E^{-4}$ mm.

Keywords: fluting medium; stress; ansys; finite element analysis; solidworks

Received: 1st June 2020

Received in revised form: 28th September 2020

Accepted: 8th October 2020

Available Online: 25th November 2020

Citation: Mohd Basri MS, Mohd Nor MZ, Shamsudin R, *et al.* Effect of different fluting medium geometrics on von-mises stress and deformation in single fluted board: a three-dimensional finite element analysis. *Adv Agri Food Res J* 2021; 2(1): a0000138. <https://doi.org/10.36877/aafrij.a0000138>

1. Introduction

Finite element-based simulation has been widely used in the last decades in performing structural analysis including stress-strain analysis (Zienkiewicz, 2004). Researchers used finite element analysis (FEA) tools in their studies including Solidworks (Slavov & Konsulova-Bakalova, 2019), Ansys (Perng *et al.*, 2020), Abaqus (Zheng *et al.*, 2020), and Catia (Río-Cidoncha *et al.*, 2020). While it is cost-effective, this "virtual prototypes" concept of recent prototyping and testing has been reliable yet accurate tool used prior to final fabrication and manufacturing process (Gallimard *et al.*, 2013).

Recent application of FEA tools including in electronics, medical equipment, packaging, and more specifically corrugated board packaging industries. The most important requirement of a package during transport and storage is the compressive strength (Csavajda *et al.*, 2017). The material and shape of the box should be able to support the product inside without damage the rest of the parts of the supported boxes. To date, most of the packaging box is corrugated and produced with a single, double or triple fluting medium (Zhang *et al.*, 2014). The shape of the fluting medium is varied and "s-shape", "ss-shape" or "UV-shape" geometry of the fluting medium is widely used.

The FEA tools have been considered to be a possible analysis and testing tool to replace the traditional yet expensive experimental methods (McKee *et al.*, 1963). This analysis tool has improved the accuracy in predicting the compression strength, stress, and total deformation of the corrugated box (Biancolini & Brutti, 2003; Gilchrist *et al.*, 1999; Rahman, 1997; Urbanik & Saliklis, 2007).

Damage of paperboard package has been studied by many researchers. Eriksson *et al.* (2014) studied the effect of concentrated load on the damage process and package collapse loads experienced by the carton board packaging. The investigation found that the damage developed at the crease and the associated peak at the force-displacement curve. The critical buckling of the orthotropic linear elastic sandwich plate has been studied by Nordstrand (2004). The simulation and experimental method have been conducted and the results showed that the governing equilibrium equations of the moment give the buckling coefficient which approaches to infinity when the aspect ratio goes to zero (Nordstrand, 2004).

In lieu of the usage of FEA tools to conduct a study on the paperboard boxes damage under compressional load, the investigations were mostly performed on the entire body of the boxes. There is limited study on the effect of different shape of fluting medium of the single fluted board on the von Mises stress and deformation due to specifically given load. Figure 1 shows the example of fluting medium in the single fluted board (A40 Packaging, 2020).

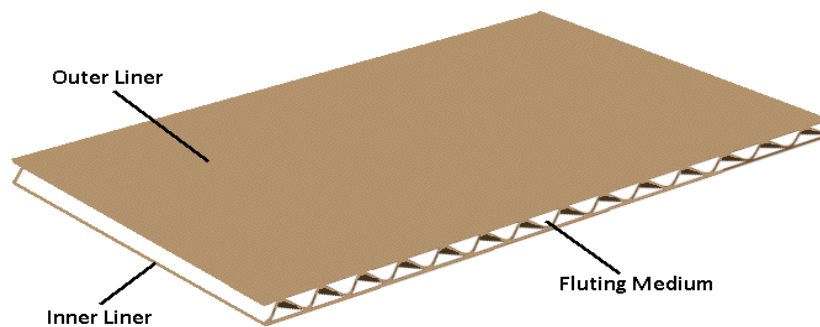


Figure 1. Parts in a single fluted board. (A40 Packaging, 2020).

The objective of this paper is to investigate the effect of different shape of the single fluted board on the von Mises stresses and deformations of the paper board. Single fluted board located at the bottom part of the box, where the maximum forces acted on them during handling and storing, will be investigated. The force on the single fluted board will be the total weight of the product stored inside the box. Since the study focusing on the stress and deformation of different shape of fluting mediums, other parameters such as temperature, independent forces, pressure and humidity will be of no interest.

2. Materials and Methods

2.1 Overview

The finite element analysis was performed using reputable and widely used commercial software, ANSYS. Prior to the static analysis, four different geometries of the fluting medium were developed using CAD software which is Solidworks. The geometries were named as s-shaped, honeycomb, triangle, and semi-circle. The shapes were selected based on its frequent selection for research purpose (Urbanik, 2001; Yuan *et al.*, 2014; Zhang *et al.*, 2014). The cross-section of the geometries is shown in Figure 2 (a)–(d).

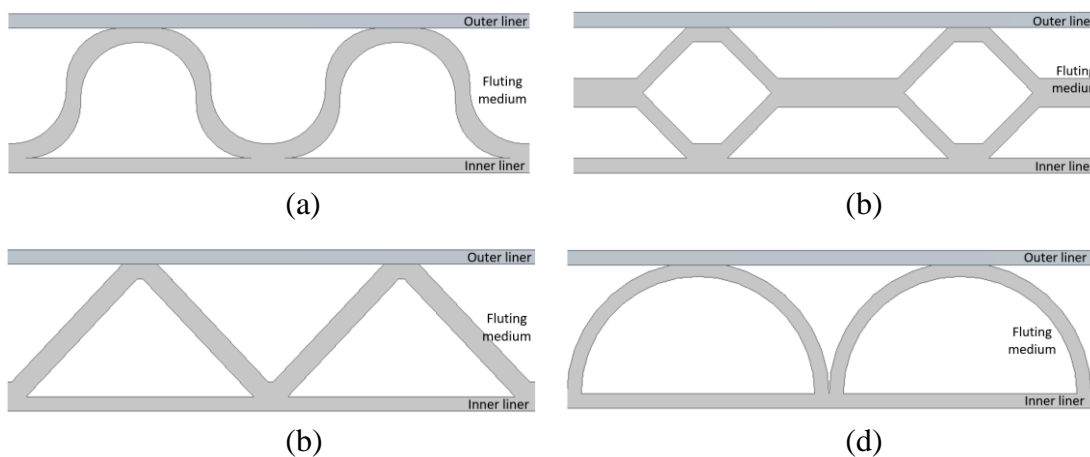


Figure 2. Geometries of the fluting mediums: (a) s-shaped, (b) honeycomb, (c) triangle, (d) semi-circle.

2.2 Materials

Materials used for the analysis is paper cardboard and the material properties are listed in Table 1 (Guang-jun *et al.*, 2009). Most of the parameters were obtained from the Solidworks material library.

Table 1. Parameters of paper cardboard.

Parameter	Value	Unit
Density	404.5	Kgm-3
Young's Modulus	8900	MPa
Poisson's Ratio	0.01	-
Bulk Modulus	3027.2	MPa
Shear Modulus	4405.9	MPa
Tensile Yield Strength	34	MPa
Compressive Yield Strength	55	MPa
Tensile Ultimate Strength	51	MPa

2.3 Load and Support

In this study, the single fluted board was subjected to static loads of 176.58 N that applied on the outer liner as shown in Figure 3. The amount of load applied was considered based on the commercial packaging box for 1.5-litre water bottles. The inner liner was considered as fixed support as shown in Figure 4.

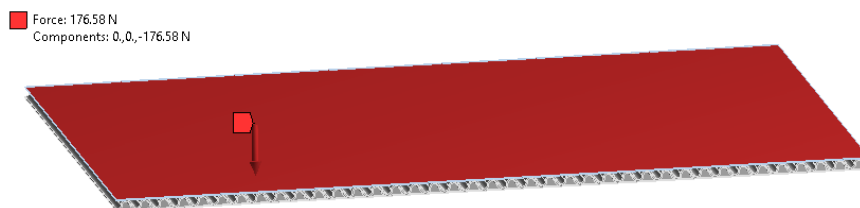


Figure 3. Static load applied on the outer liner.

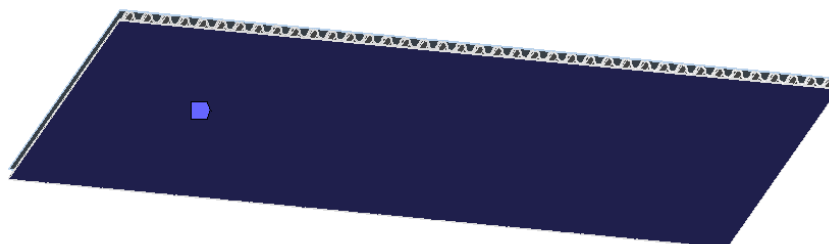


Figure 4. Fixed support on the inner liner.

2.4 Finite Element Analysis

A commercial finite element package ANSYS Workbench 2.0 Framework was used to perform the static structural analysis. The mechanical drawing of the single fluted board was drawn using Solidworks 2016 software and was imported into the ANSYS Workbench. The assembly consists of three parts including outer liner, inner liner and fluting medium as shown in Figure 1. The contact region called frictionless contact was applied between the outer liner and fluting medium (contact A) and fluting medium and inner liner (contact B). This type of contact region will depict a glue, in which the contact A and B will be allowed to slide in all directions and separated. A zero friction value is assumed between contact elements (Lee, 2018). Besides, proper boundary conditions of the outer liner, inner liner and fluting medium were defined and supported by an augmented Lagrange method and formulation. It was used since it adds an additional control of the automatically reducing the amount of penetration, so that is why it is preferred in general nonlinear problems.

Mesh convergence test was conducted on the constructed model before solving the static solutions. The mesh convergence test was performed by initially subjected the model to coarse mesh and subsequently mesh size was reduced from 15 to 4. Reducing the mesh size will result in an increasing number of nodes and solving time. An iterative analysis was carried out until results show minimal changes between iterations. The results from the mesh convergence test were selected based on the time constraint and the performance of the computer. A mesh with 71135 number of elements and 398424 number of nodes was used to mesh the model with a smooth transition as shown in Figure 5. The mesh type assigned for the model was hexagon and wedge (prism) elements. The transition ratio, maximum layers and growth rate were set at 0.272, 5 and 1.2, respectively. After obtaining the solution, the results of an analysis can be reviewed using post-processing to determine maximum induced stress and its location.

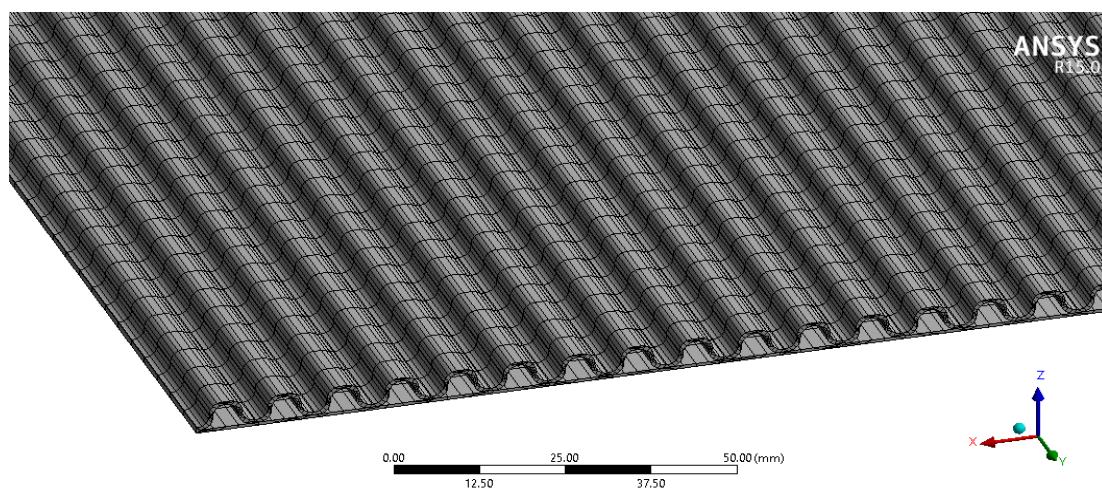


Figure 5. Meshing of the single fluted board.

2.5 Calculation of The Von-Mises Stress

The von Mises stress is effective or equivalent stress for 2D and 3D stress analysis. For a ductile material, the stress level is considered to be safe, if the von Mises stress is equal or smaller than the yield stress as shown in Equation 1, where σ_e is the von Mises stress and σ_y the yield stress of the material. This is a generalization of the 1-D (experimental) result in 2-D and 3-D situations.

$$\sigma_e \leq \sigma_y \quad (1)$$

The von Mises stress is defined by Equation 2 in which σ_1 , σ_2 and σ_3 are the three principal stresses at the considered point in a structure (Chen & Liu, 2014).

$$\sigma_e = \frac{1}{\sqrt{2}} \sqrt{(\sigma_1 - \sigma_2)^2 + (\sigma_2 - \sigma_3)^2 + (\sigma_3 - \sigma_1)^2} \quad (2)$$

For 2-D problems, the two principal stresses in the plane are determined by Equation 3 and 4.

$$\sigma_1^P = \frac{\sigma_x + \sigma_y}{2} + \sqrt{\left(\frac{\sigma_x - \sigma_y}{2}\right)^2 + \tau_{xy}^2} \quad (3)$$

$$\sigma_2^P = \frac{\sigma_x + \sigma_y}{2} - \sqrt{\left(\frac{\sigma_x - \sigma_y}{2}\right)^2 + \tau_{xy}^2} \quad (4)$$

Thus, we can also express the von Mises stress in terms of the stress components in the XY coordinate system. For plane stress conditions, it can be expressed as Equation 5.

$$\sigma_e = \sqrt{(\sigma_x + \sigma_y)^2 - 3(\sigma_x \sigma_y - \tau_{xy}^2)} \quad (5)$$

3. Results and Discussions

3.1 Overall

Results in Table 2 showed that that s-shape geometry of the single fluted board recorded the lowest von Mises stress and deformation of 0.09299 MPa and 0.00014817mm, respectively. The honeycomb geometry showed a comparable deformation of 0.00052934mm as compare to that of the s-shape geometry, however, the von Mises stress

of such geometry is doubled at 0.19576. Semi-circle and triangle geometry were found to possess high von Mises stress and deformation as compared to that of the s-shape geometry. Detail of the analysis was discussed in the following sub-sections.

Table 2. Result of the von Mises stress, deformation and strain energy.

Fluting Medium	von Mises stress (MPa)	Deformation (mm)	Strain energy (mJ)
S-shaped	0.09299	0.00014817	2.6087E-07
Semi-circle	0.13321	0.00052934	6.4500E-6
Triangle	0.15798	0.00070940	2.3431E-6
Honeycomb	0.19576	0.00018695	2.8704E-6

According to results obtained by Zhang *et al.* (2014), the maximum von Mises stress and deformation obtained were 0.0073 MPa and 0.000127×10^{-5} mm, respectively. However, the results were not comparable with this study due to several reasons including the static load applied, number of flutes in the fluting medium, flute size and arc angle. Also, results from this study may be impossible to be directly compared with other research which tested on the whole corrugated box due to dissimilar in the testing medium.

3.2 Von-Mises Stress

As it is static analysis, the Von Mises stresses acting on these fluting mediums vary according to the shape. The stresses charts are plotted as shown in Figure 6. The numerical method used for finite element analysis of the fluting mediums is Forward Difference Method.

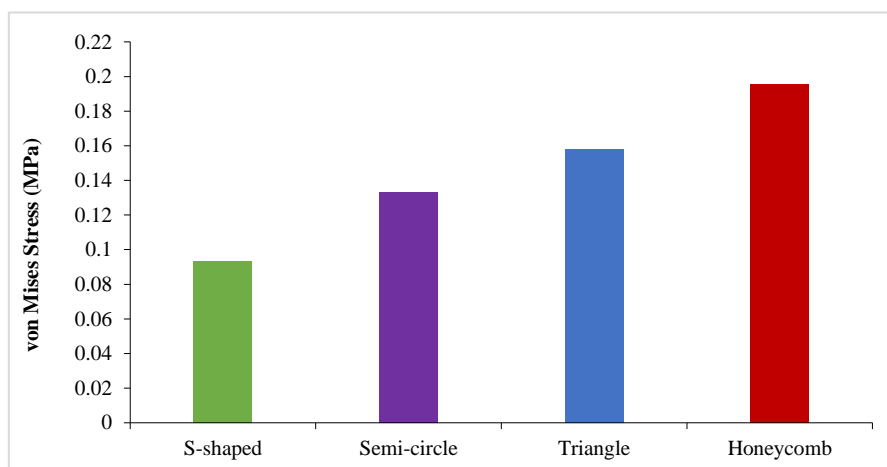


Figure 6. Von Mises stress of different fluting mediums.

Figure 7(a)–(d) clearly show the various stresses acting on different shape of fluting mediums at 10x magnification. The scale bar for the maximum and minimum von Mises

stress were set at 0.19576 MPa and automatic, respectively. The maximum von Mises stress was set based on the highest von Mises stress experienced by honeycomb shape. Most of the geometries, as shown in Figure 7(a)–(c), which has large base contact are with the inner liner has low von Mises stress. This is due to the stress load transfer directly to the inner liner thus reducing the von Mises stress experienced at the top of the fluting medium. The honeycomb geometry (Figure 7[d]) has a small direct contact area with the inner liner which resulted in less stress load transferred.

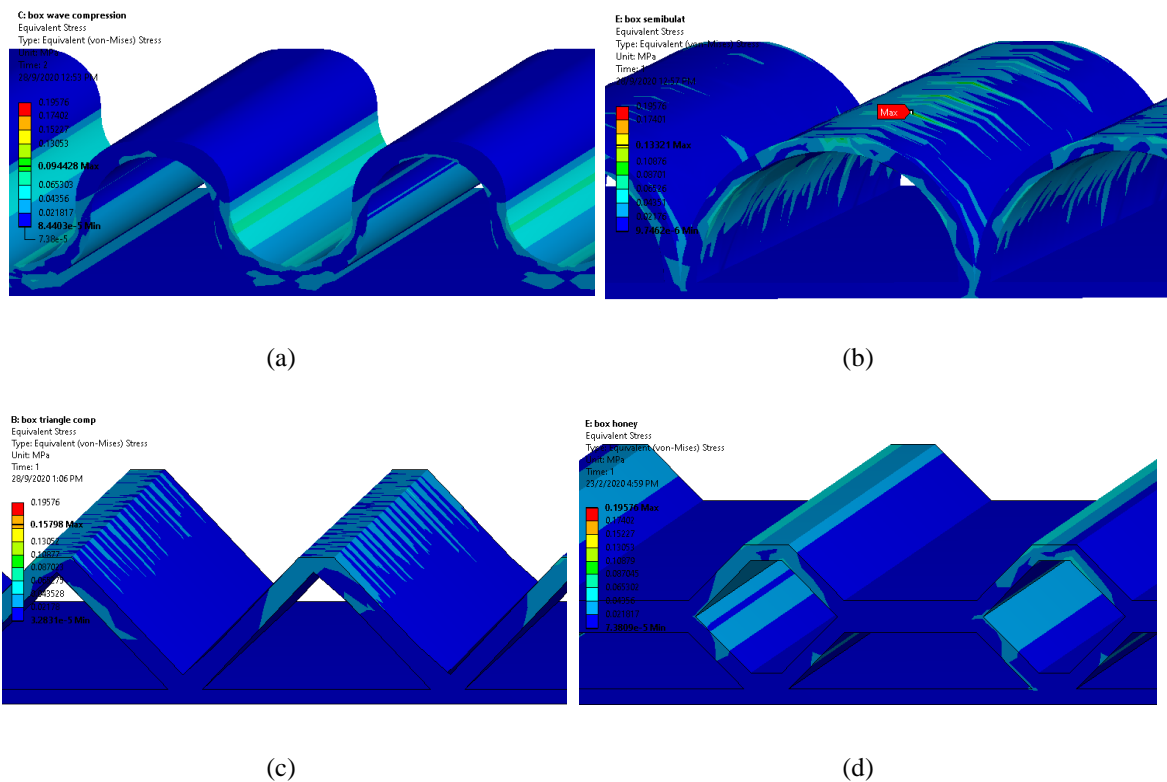


Figure 7. Stress distribution: (a) s-shaped, (b) semi-circle, (c) triangle, (d) honeycomb.

Most of the stress load is introduced at the middle part of the fluting medium and that the neutral plane shifts towards the facing on the concave side, which produces an eccentricity moment at the loaded edges. It makes the upper part of the honeycomb fluting medium become stiff and subsequently experienced the highest von Mises stress. The result is in accordance with Nordstrand *et al.* (1994). In addition, the stress of the single fluted board could be dispersed to the flute structure efficiently and then reduces the maximum stress of the board (Zhang *et al.*, 2014). In overall, all single fluted boards did not damage under given load since the von Mises stress of all boards is well smaller than the compressive yield stress of 55 MPa.

3.3 Deformation

Figure 8 shows the deformation and strain energy of different fluting medium. The deformation and strain energy were found to be related to each other. Lower strain energy

contributes to lower deformation and vice versa. In this research, the strain energy is the energy stored in a body of the single fluted board due to deformation (Sen & Awatar, 2014). When the applied force is released, the whole system returns to its original shape.

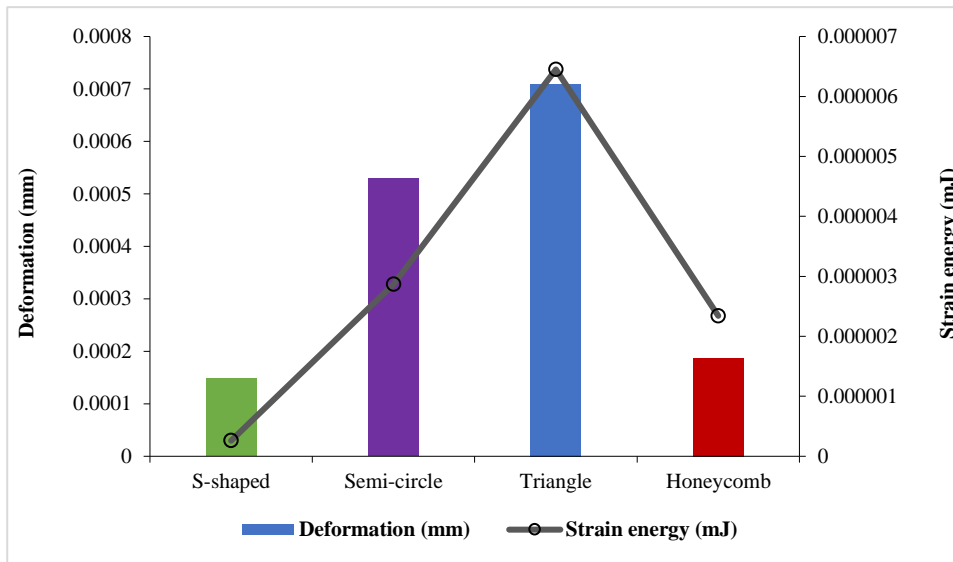
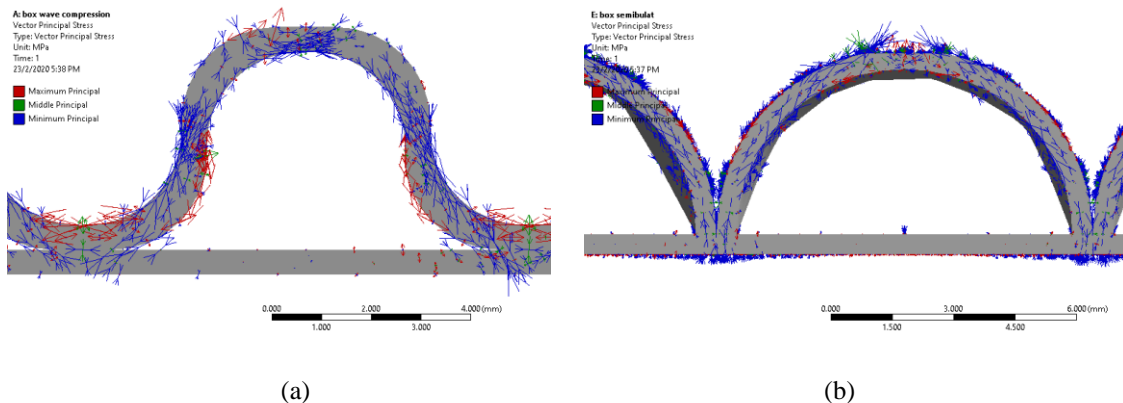


Figure 8. Deformation and strain energy of different fluting medium.

Despite its high von Mises stress, honeycomb geometry experienced comparably low strain energy and deformation. This may be probably due to its relatively high out-of-plane compression and out-of-plane shear properties. The symmetric boundary condition of s-shaped and honeycomb geometry also contributes to the strictly simultaneous collapse of the cell wall (Hou *et al.*, 2011). Figure 9(a)–(d) shows the principal stress acting on the inner liner. The triangle geometry which exhibited the highest deformation, also recorded high von Mises stress. High principal stress on the inner liner resulted in a high degree of deformation due to high strain energy generation. Figure 9(a) and (d) show very few principal stresses acting on the inner liner subsequently produce lower deformation.



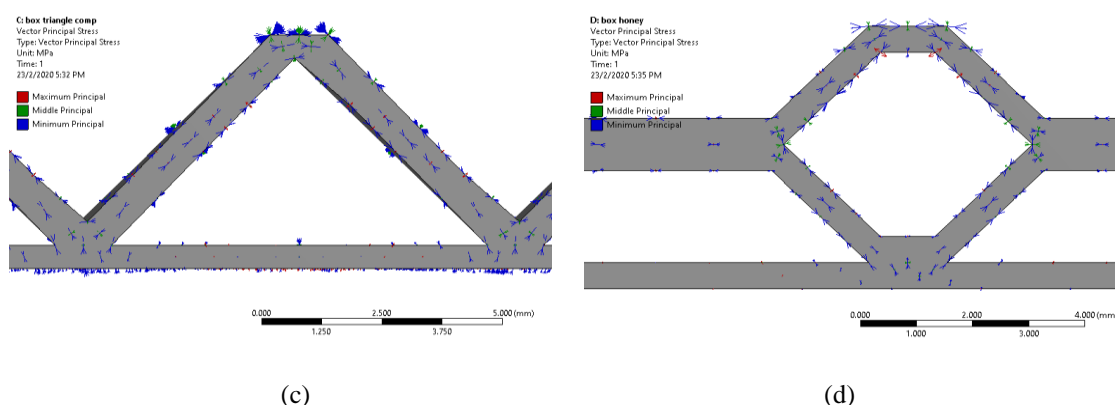


Figure 9. Principal stress acting on the inner liner of different fluting medium: (a) s-shaped, (b) semi-circle, (c) triangle, (d) honeycomb.

5. Conclusions

Based on the analyses using ANSYS software, it can be concluded that all single fluted boards did not damage under compression. The s-shaped fluting medium recorded the lowest von Mises stress and deformation at 0.09299 MPa and 0.00014817 mm, respectively. The highest von Mises stress and deformation were experienced by honeycomb and triangle geometries, respectively. The finite element analysis tool was found to be reliable in investigating the effect of the different design of the fluting medium on the von Mises stress and deformation. For future studies, orthotropic or anisotropic behavior study and dynamic analysis with deformation order of at least 5–10% onwards are recommended.

Author Contributions: Conceptualization, M.S.M.B. and I.S.M.A.T.; methodology, M.Z.M.N. and R.S.; software, N.H.A.G. and K.M.K.; validation, I.S.M.A.T. and A.M.M.; formal analysis, A.M.M.; writing—original draft preparation, M.S.M.B.; writing—review and editing, M.Z.M.N. and N.H.A.G.

Acknowledgments: The authors would like to thank individuals in UPM and Institutes for your involvement.

Conflicts of Interest: The authors declare no conflict of interest.

References

- A40 Packaging. (2020). Board Grades. Retrieved from <https://www.a40packaging.co.uk/boardgrades.php>
- Biancolini, M., & Brutti, C. (2003). Numerical and experimental investigation of the strength of corrugated board packages. *Packaging Technology and Science: An International Journal*, 16(2), 47–60.
- Chen, X., & Liu, Y. (2014). *Finite element modeling and simulation with ANSYS Workbench*: CRC press.
- Csavajda, P., Böröcz, P., Mojzes, Á., et al. (2017). The effect of creasing lines on the compression strength of adjustable height corrugated boxes. *Journal of Applied Packaging Research*, 9(1), 15–22.
- Eriksson, D., Korin, C., & Thuvander, F. (2014). *Damage to carton board packages subjected to concentrated loads*. Paper presented at the 19th IAPRI World Conference on Packaging, Melbourne, Australia, June 15–18, 2014.

- Gallimard, L., Vidal, P., & Polit, O. (2013). Coupling finite element and reliability analysis through proper generalized decomposition model reduction. *International journal for numerical methods in engineering*, 95(13), 1079–1093.
- Gilchrist, A., Suhling, J., & Urbanik, T. (1999). Nonlinear finite element modeling of corrugated board. *Mechanics of Cellulosic Materials*, 85,101–106.
- Guang-jun, H., Xiang, H., & Wei, F. (2009). Finite element modeling and buckling analysis of corrugated box. *Packaging Engineering*, 30(3), 34–35.
- Hou, B., Pattofatto, S., Li, Y., *et al.* (2011). Impact behavior of honeycombs under combined shear-compression. Part II: Analysis. *International Journal of Solids and Structures*, 48(5), 698–705.
- Lee, H. H. (2018). *Finite element simulations with ANSYS Workbench 18*: SDC publications.
- McKee, R., Gander, J., & Wachuta, J. (1963). Compression strength formula for corrugated boxes. *Paperboard packaging*, 48(8), 149–159.
- Nordstrand, T. (2004). On buckling loads for edge-loaded orthotropic plates including transverse shear. *Composite structures*, 65(1), 1–6.
- Nordstrand, T., Carlsson, L. A., & Allen, H. G. (1994). Transverse shear stiffness of structural core sandwich. *Composite structures*, 27(3), 317–329.
- Perng, J. W., Kuo, Y. C., Chang, Y. T., *et al.* (2020). Power substation construction and ventilation system co-designed using particle swarm optimization. *Energies*, 13(9), 1–27.
- Rahman, A. A. (1997). Finite element buckling analysis of corrugated fiberboard panels. *ASME Applied Mechanics Division-Publications-AMD*, 221, 87–92.
- Río-Cidoncha, D., Rojas-Sola, J. I., & González-Cabanes, F. J. (2020). Computer-aided design and kinematic simulation of Huygens's pendulum clock. *Applied Sciences*, 10(2), 1–27.
- Sen, S., & Awtar, S. (2014). Nonlinear strain energy formulation of a generalized bisymmetric spatial beam for flexure mechanism analysis. *Journal of Mechanical Design*, 136(2), 1–13.
- Slavov, S., & Konsulova-Bakalova, M. (2019). Optimizing weight of housing elements of two-stage reducer by using the topology management optimization capabilities integrated in SOLIDWORKS: A case study. *Machines*, 7(1), 1–15.
- Urbanik, T. (2001). Effect of corrugated flute shape on fibreboard edgewise crush strength and bending stiffness. *Journal of Pulp and Paper Science*, 27(10), 330–335.
- Urbanik, T. J., & Saliklis, E. P. (2007). Finite element corroboration of buckling phenomena observed in corrugated boxes 1. *Wood and fiber science*, 35(3), 322–333.
- Yuan, W., Sun, J. X., Zhang, G. M., *et al.* (2014). Corrugated board UV flute-shaped structure size optimization design based on the finite element. *Applied Mechanics and Materials*, 469, 213–216.
- Zhang, Z., Qiu, T., Song, R., *et al.* (2014). Nonlinear finite element analysis of the fluted corrugated sheet in the corrugated cardboard. *Advances in Materials Science and Engineering*, 1–9.

Zheng, L., Chen, W., & Huo, D. (2020). Investigation on the tool wear suppression mechanism in non-resonant vibration-assisted micro milling. *Micromachines*, 11(4),1–17.

Zienkiewicz, O. (2004). The birth of the finite element method and of computational mechanics. *International journal for numerical methods in engineering*, 60(1), 3–10.



Copyright © 2021 by Mohd Basri MS *et al.* and HH Publisher. This work is licensed under the Creative Commons Attribution-NonCommercial 4.0 International License (CC-BY-NC4.0)